

# All-optical in-situ analysis of PIAD deposition processes

Steffen Wilbrandt, Olaf Stenzel, Norbert Kaiser  
Fraunhofer IOF, Albert-Einstein-Str. 7, 07745 Jena, Germany

## ABSTRACT

In the case of plasma ion assisted deposition (PIAD) processes either quartz crystal monitoring or optical monitoring are commonly applied to control thickness of the layers.

For several oxide layer materials the final stoichiometry of the deposited film is extremely sensitive to the oxygen gas inlet during the deposition process. It is well known, that under these circumstances, variations in the reaction gas flow or in deposition rates may cause unwanted variations of the stoichiometry of the coating. Finally this results in film inhomogeneities and increased absorption losses, which cannot be identified early enough and reliably by in-situ transmission spectroscopy alone. For this reason, the correlation between optical performance of the coating and emission spectra of the APS-plasma measured by a separate analyzer has been investigated. The synchronization in recording in-situ transmission spectra and plasma emission spectra was achieved by developing a common trigger unit for both spectrum analyzers.

From the correlation between spectrophotometry and emission spectroscopy, we expect an earlier and more reliable assignment of absorption losses and inhomogeneities to instabilities in the process parameters of the deposition process.

**Keywords:** interference coatings, optical monitoring, plasma emission spectroscopy, absorption, film inhomogeneity

## 1. INTRODUCTION

The in-situ measurement of transmission spectra of a growing optical coating on the rotating substrate holder has established itself as a standard technique in the last years [1-5]. In a first scenario when optical constants and all other model parameters (roughness, inhomogeneities, parallel interfaces, ...) consistent with what is assumed in the design, in-situ monitoring is often used to identify deposition termination points and thus to control the deposition process [1-3]. If not, a second scenario in-situ monitoring allows to detect deviations of the spectral performance of the growing coating from what has been designed, and thus to define suitable correction strategies if possible [4].

The present paper deals with the second of these two scenarios. A weak point of the approaches existing so far is the correct assignment of deviations in the in-situ transmission to their concrete origin. Thus, a downshift in transmittance may be caused by a film inhomogeneity (positive index gradient) as well as by optical losses (absorption or scattering). To distinguish between these cases would require at least one second measurement, for example a reflectance measurement at the same sample position.

Although development work on in-situ reflectance measurements of samples on the rotating substrate holder is a matter of current projects, it will still take some time until corresponding ready-to-use measurement setups will be commercially available. On the other hand, it is well known that changes in oxygen concentration during oxide layer deposition will result in stoichiometry changes in the coating, thus having an influence on both refractive index and extinction of the coating. In Plasma Ion Assisted Deposition (PIAD) processes, changes in oxygen gas concentration are principally detectable by means of plasma emission spectroscopy. The purpose of this paper is therefore to report on coating deposition process control by parallel optical broadband monitoring of the growing film and optical emission spectroscopy of the plasma.

Fig. 1 visualizes possible application directions of this complex of in-situ measurement techniques.

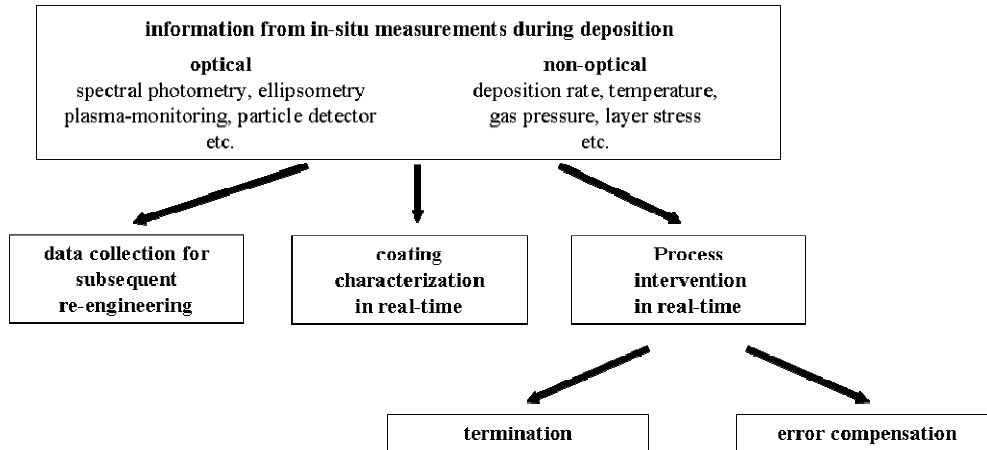


Fig. 1 Overview of in-situ information and its utilization in the deposition process

According to Fig. 1, all optical in-situ techniques (those discussed here and others like in-situ ellipsometry [6,7] and so on [8]) may be used for different purposes. The first one includes pure data collection and archiving for later evaluation if necessary. In this case the in-situ analysis is completely passive during deposition.

A second possibility, which requires fast calculation routines, pursues the real time coating characterization from in-situ measurement results. This may be used for permanent process control, but the control unit still remains passive as long as all data are consistent with what is expected from the design. Active process intervention may occur when in-situ measurements are used for deposition termination point determination. Another active intervention includes active error compensation, when deposition errors have been identified from in-situ measurements, and shall be compensated by changes in deposition parameters or design modifications, if possible. In this study, we will focus on real time re-engineering from optical data (optical broadband monitoring and optical emission spectroscopy of the plasma).

## 2. EXPERIMENTAL

Fig. 2 shows the principal experimental setup.

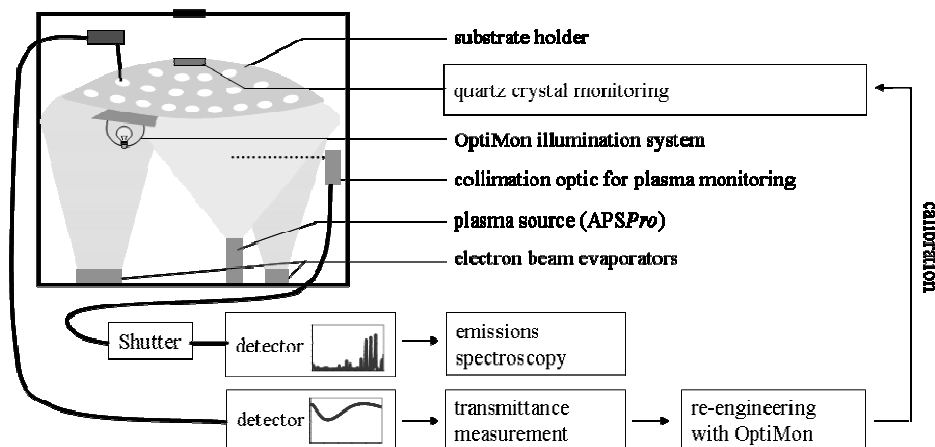


Fig. 2: Integration of optical measurements into the deposition chamber: Principal scheme

The experiments are performed in a Leybold Syrus Pro 1100 deposition system equipped with two electron beam evaporators and the Advanced Plasma Source APSPPro. In-situ transmission spectroscopy is performed in a wavelength range between 400nm and 920nm by means of the OptiMon system [9]. The OptiMon system is equipped with a CCD detector for recording 100% reference  $I_{100\%}$ , dark spectrum  $I_{\text{dark}}$  and sample spectrum

$I_{\text{sample}}$  per one rotation of the sample holder. From these spectra, the CCD-detector calculates the intensity of the light source  $I_{\text{light source}}$  via:

$$I_{\text{light source}}(\lambda) = I_{100\%}(\lambda) - I_{\text{dark}}(\lambda) \quad (1)$$

and the transmittance  $T_{\text{CCD}}$  via:

$$T_{\text{CCD}}(\lambda) = 1000\% \frac{I_{\text{sample}}(\lambda) - I_{\text{dark}}(\lambda)}{I_{100\%}(\lambda) - I_{\text{dark}}(\lambda)} \quad (2)$$

where the intensities  $I$  are the digitalized (15-bit resolution), during the integration time accumulated analog outputs of the CCD-array for a certain pixel, which corresponds to a single wavelength. To achieve good measurement accuracy it is important to keep the influence of intensity fluctuations of the halogen bulb between these measurements small. In the OptiMon-system we not only use a very stable power supply, the 100% reference will be also measured only ~120ms before the sample measurement is performed.

It should be emphasized that the illumination is performed by means of an Ulbricht sphere (glass-ceramic) located in the deposition chamber, the illumination optics withstands deposition temperatures up to 300°C. In the case of deposition temperatures below 100°C we use a BaSO<sub>4</sub>-coating for the Ulbricht sphere, which allows measurement down to 360nm with acceptable noise level, even when a 5W (instead of a 35W) halogen bulb is used.

The light emitted by the APS plasma is collected from a rather small (selectable) spatial region and guided to a second detector, which is synchronized to the transmission measurement in order to correlate recorded emission data to the relevant transmission spectra. As indicated in Fig.2, both measurements are spatially separated from each other, so that the transmission light detector is well shielded from plasma emission, while the light source for transmission measurement does not influence the plasma emission measurement. However, the emission measurement will detect a disturbing background signal from electron beam guns, which is discussed in Sect.3.2.

Technical details are given in Tab.1

	OptiMon	PlasmaMonitor
<b>spectral range</b>	<b>360-920nm</b>	<b>200-850nm</b>
<b>slit</b>	<b>140µm</b>	<b>50µm</b>
<b>optical resolution</b>	<b>~5nm</b>	<b>~2nm</b>
<b>typical integration time</b>	<b>4ms</b>	
<b>CCD array</b>	<b>Hamamatsu S9840 (2048 x 14 active pixel, pixel size 16µm x 16µm)</b>	
<b>PC interface</b>	<b>USB, RS485 @921600 bit/s</b>	
<b>2-bit trigger interface</b>	<b>00 no measurement</b> <b>01 dark measurement</b> <b>11 reference measurement</b> <b>10 transmittance measurement</b>	

Tab.1: technical details of the detectors for transmission measurement (OptiMon) and plasma emission measurement (PlasmaMonitor)

### 3. DATA AKQUISITION AND PROCESSING

#### 3.1 In-situ transmittance

The OptiMon measurement unit is connected to the OptiMon software environment that includes several options for data acquisition and powerful re-engineering algorithms for multilayer stacks. The re-engineering software library has been developed by the group of Alexander Tikhonravov at Moscow State University. The general interplay philosophy between the mentioned units is sketched in Fig. 3:

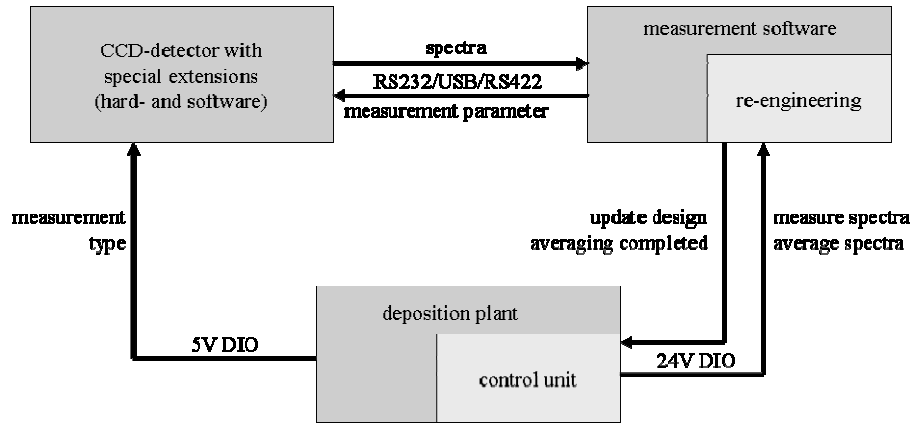


Fig.3 Schematic presentation of the interplay between hard- and software units

Basically, the deposition plant must provide a 2-bit trigger interface to the CCD-detector to request intensity measurements. Each time when such a request occurs, the detector starts a measurement using the most recent settings (wavelength range, integration time, parameters for internal smoothing, ...) provided by the measurement software. After completing a measurement of the 100% reference, the intensity of the light source is calculated by eq. (1) and transferred to the measurement software via serial communication. In the case of completing the measurement of the sample intensity, the CCD-detector applies eq. (2) and calculates a series of integer numbers for the transmittance in units of one-tenth of a percent and sends this data to the measurement software.

The illumination optic of the OptiMon-system contains a gain-flattening-filter to achieve a nearly constant intensity of the light source for the complete spectral range. In this case, the following equation for the transmittance  $T_{\text{meas}}$  with particular compensation of the nonlinear response of the CCD can be deducted:

$$T_{\text{meas}}(\lambda) = \frac{\sqrt{1 - qT_{\text{CCD}}(\lambda)} - 1}{\sqrt{1 - q} - 1} \quad (3)$$

For this compensation only the transmittance  $T_{\text{CCD}}$  calculated by equation (2) and a single parameter  $q$  to quantify the non-linearity are required. When applying this equation to 0% and 100% transmittance values, the non-linearity has no effect. On the other hand, transmittance values close to 50% could be strongly influenced by the nonlinear behavior of the detector. In the case of our CCD-detector the parameter  $q$  was determined to be approximately 0.08. This corresponds to a 0.5% increased transmittance value for a sample with 50% transmittance. In the data sheet of the CCD-array the non-uniformity at the half of the full well capacity output is outlined to be typically 3% and guaranteed to be below 10% [10]. When the limiting of the gain-flattening-filter to the intensity of the light source to one third of the available dynamic range of the CCD-array is taken into account, the observed non-linearity is as expected. This pre-processing of the transmittance data is applied in the measurement software before re-engineering starts. Furthermore, cross talk between pixels in the CCD-array caused by charge transfer in the CCD-array [11] or limited spectral resolution could be optionally modeled during the calculation of theoretical spectra. Numerous measurements on different calibration samples have shown that further systematic errors of the OptiMon system could be neglected and reliable coating characterization is possible [12].

It is a key feature of the used re-engineering software that the optical constants of the growing film are supposed to be known in advance and remain fixed, while the film thickness values are optimized in order to fit measured transmission spectra. The feasibility of this approach has been tested by a series of deposition runs of single layers. For typical oxides, relative variations in refractive indices from experiment to experiment were of the order of 0.1% (standard deviation), while relative thickness variations were between 0.9% (for  $\text{Ta}_2\text{O}_5$ ) and 1.5% (for  $\text{SiO}_2$ ).

There are two basic modes for data acquisition and re-engineering (compare Fig. 4):

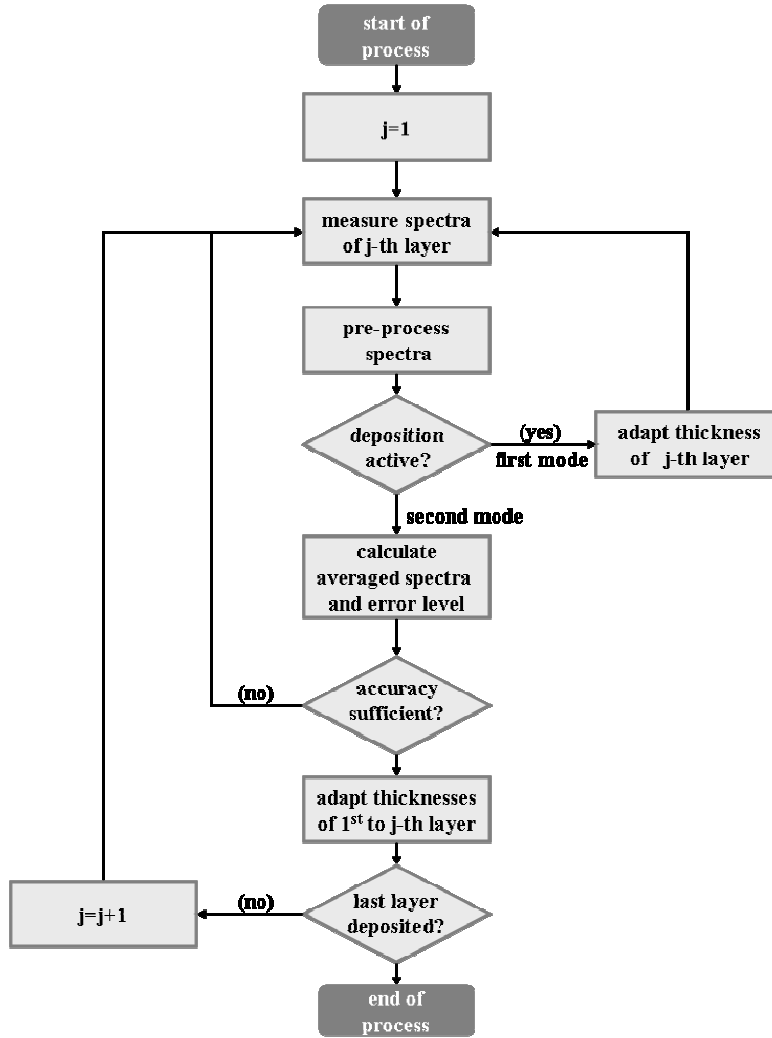


Fig. 4 Flow chart of the operation modes for data acquisition and re-engineering

**First mode:** permanent thickness calculation for the active ( $j$ -th) layer: Imagine that the deposition of the  $j$ -th layer is in progress. In this mode, the re-engineering software will permanently calculate the thickness  $d_j^S$  of the  $j$ -th layer, keeping the thickness values  $d_1, \dots, d_{j-1}$  for the previously deposited layers (if they exist) constant. This is the so called sequential re-engineering algorithm and the thickness calculation is performed by minimizing the (so-called sequential) merit function  $F_s(d_j^S)$ :

$$F_s(d_j^S) = \left[ \frac{1}{N} \sum_{i=1}^N \left( \frac{T_{\text{meas}}^{S(j)}(\lambda_i) - T_{\text{calc}}^{S(j)}(\lambda_i, d_1, \dots, d_{j-1}, d_j^S)}{\Delta T_s(\lambda_i)} \right)^2 \right]^{\frac{1}{2}} \quad (4)$$

This mode allows rapid calculation, because only one (the latest calculated by eq. (3)) spectrum  $T_{\text{meas}}^{S(j)}$  containing  $N$  spectral points is used to calculate only one thickness.  $T_{\text{calc}}^{S(j)}$  is the calculated transmittance for the deposited layer stack and  $\Delta T_s$  is the transmittance measurement error for sequential mode. In the present version of the OptiMon software it will be loaded from an external file. Often, only this mode is implemented into re-engineering software and propagation of thickness errors could be a problem [13]. For this reason the OptiMon software additionally implements a second mode.

**Second mode:** Calculation of the thickness values for all deposited layers by a full triangular algorithm [14]. In this mode, the average of all transmission spectra, *which have been recorded in the break after the deposition of a particular layer of the design has been completed and the deposition of the next one has not yet started*, are included into the calculation. Thereby, averaging individual spectra  $T_{\text{meas}}^{\text{T}(i)}$  (total number of spectra  $L$ ) by the measurement software will continued until the estimated error level  $\Delta T_{\text{E}}$ , calculated by the following equation

$$\Delta T_{\text{E}}(\lambda) = \left\{ \frac{1}{L(L-1)} \left[ \sum_{i=1}^L \left( T_{\text{meas}}^{\text{T}(i)}(\lambda) \right)^2 - \frac{1}{L} \left( \sum_{i=1}^L T_{\text{meas}}^{\text{T}(i)}(\lambda) \right)^2 \right] \right\}^{\frac{1}{2}} \quad (5)$$

is for all wavelength lower than a predefined threshold (commonly 0.25%).

Obviously, the first transmission spectrum  $T_{\text{meas}}^{\text{T}(1)}$  is recorded when the first layer has been deposited, it depends only on the thickness of the first layer. The second spectrum  $T_{\text{meas}}^{\text{T}(2)}$  already depends on two thickness values and so on. The full triangular re-engineering algorithm is to determine all thickness values instantaneously by fitting all those transmission spectra by the corresponding theoretical spectra  $T_{\text{calc}}^{\text{T}(j)}$ . So the thickness calculation is performed by minimizing the (so-called triangular) merit function [14]:

$$F_{\text{T}}^{(j)}(d_1, \dots, d_j) = \left[ \frac{1}{JN} \sum_{j=1}^J \sum_{i=1}^N \left( \frac{T_{\text{meas}}^{\text{T}(j)}(\lambda_i) - T_{\text{calc}}^{\text{T}(j)}(\lambda_i, d_1, \dots, d_j)}{\Delta T_{\text{T}}(\lambda_i)} \right)^2 \right]^{\frac{1}{2}} \quad (6)$$

Any new recorded spectrum may therefore, in principle, lead to changes in the calculated thickness values of the previously deposited layers.  $\Delta T_{\text{T}}$  is the transmittance measurement error for the triangular mode and it will be estimated by:

$$\Delta T_{\text{T}}(\lambda) = \Delta T_{\text{E}}(\lambda) \sqrt{L} = \left\{ \frac{1}{L-1} \left[ \sum_{i=1}^L \left( T_{\text{meas}}^{\text{T}(i)}(\lambda) \right)^2 - \frac{1}{L} \left( \sum_{i=1}^L T_{\text{meas}}^{\text{T}(i)}(\lambda) \right)^2 \right] \right\}^{\frac{1}{2}} \quad (7)$$

In practice, the second mode is applied for thickness calculation in the evaporation break after the completion of (say the  $(j-1)$ th) layer. For convenience, the break is used to accumulate spectra until an acceptable minimum noise level is achieved. The thus averaged transmission spectrum is included into the set of spectra fitted by means of the triangular algorithm. As the result, the  $j-1$  thickness values of the already deposited layers are calculated. If they are deviating from the intended thickness values, they may be used for quartz crystal recalibration or, if necessary, for error compensation by thickness reoptimization of the not yet deposited layers of the design. Future automation of this procedure would be only requiring an additional interface between measurement software and deposition plant to update the thickness of the next layer (fig. 3).

During subsequent deposition of the  $j$ -th layer, the OptiMon system again operates in the first mode, until this layer is completed and OptiMon switches back to the second mode and so on. Thereby, the information required to select the proper operation mode in the measurement software must provided by the deposition plant (fig. 3).

### 3.2 Plasma emission spectroscopy

The CCD-detector used for plasma emission spectroscopy is similar to the one used for measurements of the in-situ transmittance. As already outlined in table 1, for plasma emission spectroscopy an extended spectral range and a higher spectral resolution is used. The trigger interface in both detectors is identical, but the provided signal sequences from the deposition plant are different:

Due to the negligible drift of the dark signal during typical process, the dark signal is only measured before starting the deposition and assumed to be constant. In principle, also a continuous dark signal measurement could be implemented, requiring an additional shutter in front of the detector (see figure 2). During the deposition process only measurements of the reference signal are requested by the plant. After these measurements are completed, the CCD-detector performs the calculation of the emission spectrum by equation

(1) and transfers it to the measurement software via serial communication. The subsequent spectra analysis includes identification of spectral lines using SpecLine-software provided by Plasus [15].

A serious problem during measurements of the plasma emissions could be the background light generated by operation of electron beam evaporators. This background intensity is not constant because the emission current of the electron beam guns and reflectivity of the chamber sheets change during the deposition process (figure 5). In the present configuration the background signal is minimized by shadowing blades.

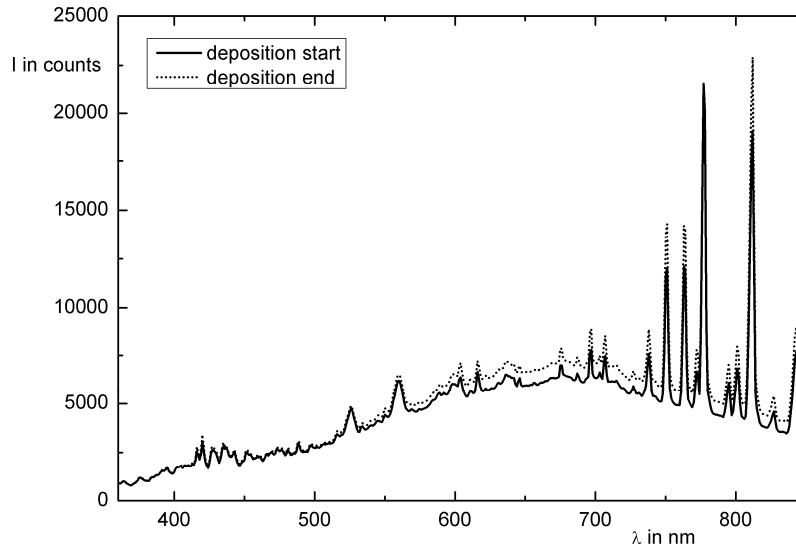


Fig. 5 Measured spectrum during APS-assisted evaporation of tantalum pentoxide as superposition of discrete plasma lines (narrow spikes) and background from electron beam guns (broad structure), when working without shadowing blades.

#### 4. RESULTS AND DISCUSSION

In the present section we will mainly present an example on the different information content of in-situ plasma emission spectra and transmission spectra. We will present a very simple example: the deposition of a 200nm thick niobium oxide film on fused silica. The APS-plasma emission spectrum is then composed from a variety of emission lines mainly originating from electronic transitions in atomic and ionic argon and oxygen. A part of such a spectrum is shown in Fig. 6. Although the electron beam evaporator was active during the measurement, the corresponding background signal is nearly completely eliminated here.

In order to visualize the most characteristic oxygen emission line at 777nm, the experiment has been performed with two different oxygen flow values while keeping all other parameters constant: with high oxygen flow in order to obtain a good transparent stoichiometric niobium pentoxide film (dashed spectrum), and with a low oxygen flow (solid line), which is expected to result in an understoichiometric film with high absorption losses. The relevant deposition parameters are outlined in Tab. 2. As seen from Fig. 6, the lack in oxygen during deposition may be immediately identified in the emission spectrum, because of the strong changes in the relative intensity of the oxygen line at 777nm.

	Stoichiometric niobium pentoxide	Understoichiometric niobium pentoxide
Argon flow	14 sccm	
Oxygen flow	30 sccm	20 sccm
Deposition rate	0.5 nm/s	
Bias voltage	110 V	
Substrate temperature	100 °C	

Tab. 2 Deposition parameter for preparation of the niobium oxide films on fused silica

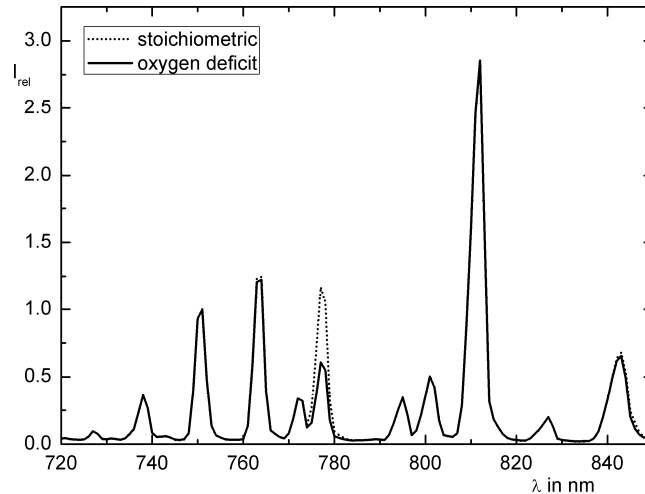


Fig. 6 Normalized APS plasma emission spectra during deposition of a niobium oxide film with two different values of the oxygen flow (compare Tab.2)

In the case of in-situ transmission spectroscopy it is obvious that a certain minimum thickness will be required in order to identify the absorption losses in the understoichiometric film from transmission measurements. Fig. 7 shows the transmission spectra of both films at a thickness of approximately 15nm, and at the end of the deposition. It is obvious that the understoichiometric film is strongly absorbing, but nevertheless a clear identification of a deviation from the expected behavior is only possible at thicknesses above approximately 15nm. A very thin but absorbing film can still be fitted assuming optical constants of stoichiometric niobium pentoxide, but with a wrong film thickness.

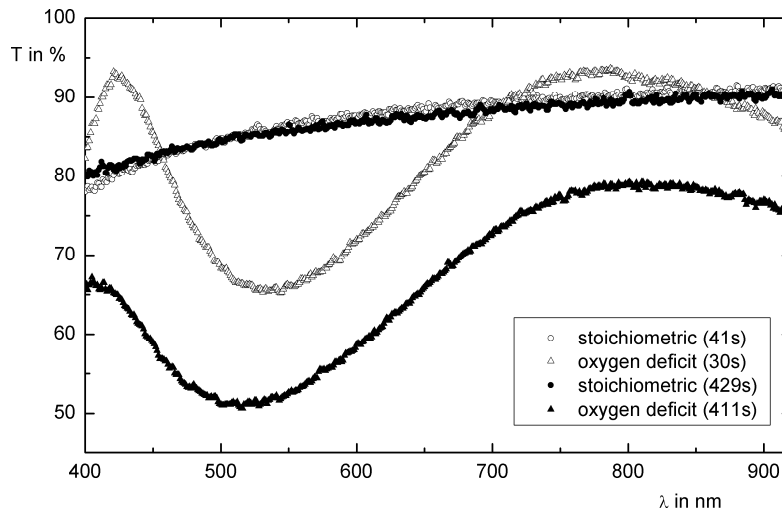


Fig. 7: in-situ transmission spectra:

stoichiometric niobium pentoxide film (circle):		
at deposition time 41s (hollow):	$d_{\text{optimon}}=17.0\text{nm}$	$d_{\text{quartz}}=12.8\text{nm}$
at deposition time 429s (filled):	$d_{\text{optimon}}=174.5\text{nm}$	$d_{\text{quartz}}=170.0\text{nm}$
understoichiometric (oxygen deficit) niobium pentoxide film (triangle)		
at deposition time 30s (hollow):	$d_{\text{optimon}}=17.6\text{nm}$	$d_{\text{quartz}}=11.1\text{nm}$
at deposition time 411s (filled):	$d_{\text{optimon}}=54.1\text{nm}$	$d_{\text{quartz}}=170.0\text{nm}$

This is visualized in Figs. 8 and 9. During deposition of the film, OptiMon operates in the first data processing mode, calculating the film thickness during deposition by minimizing the merit function according to Eq. (4) while using the optical constants of the stoichiometric niobium pentoxide. Fig. 8 shows the thus calculated film thickness as a function of deposition time. While in the case of correct oxygen flow (dot), the calculated thickness grows linearly in time, the deposition failure with understoichiometric niobium pentoxide (solid line) becomes obvious from thickness calculation approximately after 120 seconds. But after these 120 seconds, almost 60nm of the absorbing niobium oxide are deposited, resulting in an absorption which is clearly too strong for any reasonable application as interference coating. So that this charge would clearly be wasted.

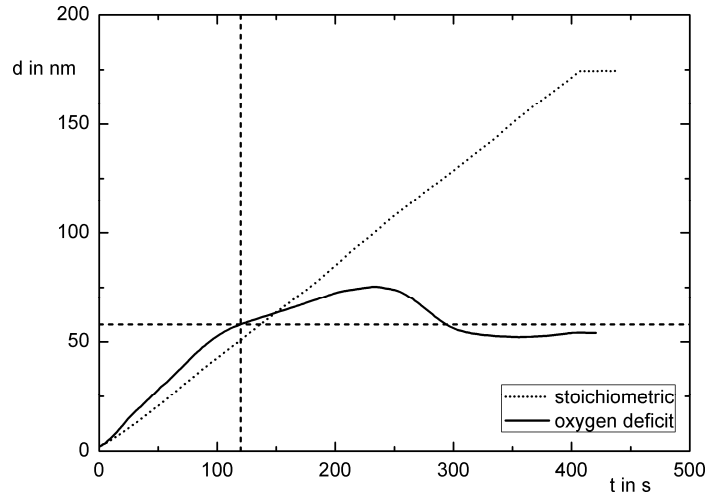


Fig. 8 niobium oxide film thickness as function of deposition time calculated from in-situ transmission by minimizing merit function (eq. (4)) assuming optical constants of stoichiometric niobium pentoxide: dot: stoichiometric film; solid – understoichiometric film. The dashed straight lines indicate the threshold where deviations in the behavior of the understoichiometric film from the expected behavior become clearly obvious.

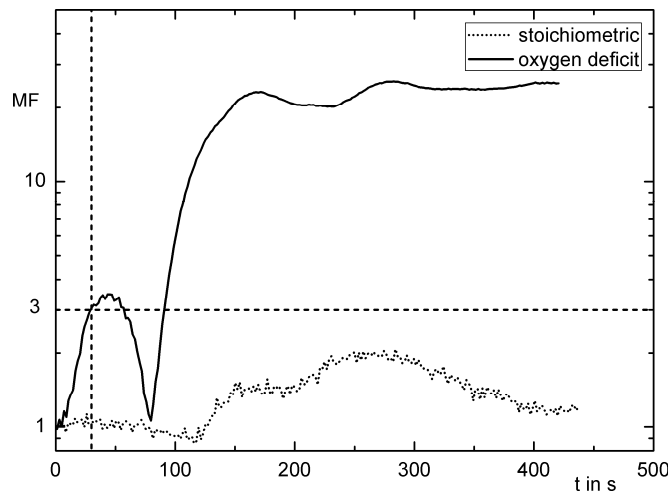


Fig. 9 calculated value of the merit function MF (eq. (4)) as function of deposition time assuming optical constants of stoichiometric niobium pentoxide: dot: stoichiometric film; solid – understoichiometric film. The dashed straight lines indicate the threshold where deviations in the behavior of the understoichiometric film from the expected behavior become clearly obvious.

The situation becomes more encouraging when the merit of the in-situ spectra fit is taken into account. Fig. 9 shows the calculated merit function according to Eq. (4) for both experiments, again as a function of deposition time. For stoichiometric niobium pentoxide, the fit is excellent over the entire deposition time, resulting in a very low merit function (note the logarithmic scale in Fig.9). On the contrary, the understoichiometric niobium pentoxide is well fitted (although with a wrong thickness) for very thin layers. But approximately after 30 seconds, the merit function exceeds a value which is attributed to a clearly identifiable fitting discrepancy (dashed horizontal line), so that the operator will recognize that the deposition goes wrong. Nevertheless, even in this case, there is already a thickness of approximately 15nm deposited, resulting in an absorption loss of approximately 2%. Commonly, even a multilayer stack containing only a single coating with such high absorption loss will not fulfill the specification.

On the contrary, the plasma emission spectra (Fig. 6) give clear indication on the oxygen lack from the very beginning of the deposition experiment.

Certainly this example is very simple, but its function is to show that in-situ transmission spectra alone may fail in identifying deposition errors early enough in order to escape a wrong-going deposition charge. A combination of in-situ transmission with other in-situ optical data such as emission spectra will be extremely useful in order to enhance the significance of in-situ optical spectroscopy results.

## 5. SUMMARY

We have demonstrated hard- and software tools for synchronized recording of in-situ transmission spectra of the growing film and emission spectra of the APS plasma during PIAD deposition processes of oxide interference layers. It could be shown that these spectra deliver complementary information, and that their combination allows faster and more reliable detection of deposition errors at an early stage of film deposition. Particularly, the emission spectra may deliver information on impending film understoichiometry and thus enhanced absorption. Future work will focus on the implementation of reflectance measurements on the rotating substrate holder in order to achieve an all-optical in-situ analysis of the deposition process.

## 6. ACKNOWLEDGMENTS

The authors are grateful to Alexander Tikhonravov and Michael Trubetskov (Moscow State University) for providing the library for re-engineering, and to Heidi Haase (Fraunhofer IOF Jena) for technical assistance.

Financial support of the BMWi, Germany, as supplied in terms of the TACo-grant is also gratefully acknowledged.

## 7. REFERENCES

- [1] D. Ristau, H. Ehlers, T. Gross, M. Lappschies, "Optical broadband monitoring of conventional and ion processes", *Appl. Opt.* 45 (2006), 1495
- [2] A. Zöllner, "Direct optical monitoring on the rotating substrate holder", *VIP 19 Nr.3* (2007), 6
- [3] B. Badoil, F. Lemarchand, M. Cathelinaud, M. Lequime, "Interest of broadband optical monitoring for thin filter manufacturing", *Appl. Opt.* 46 (2007), 4294
- [4] [http://www.evatecnet.com/sites/pdf/EVATEC\\_GSM1100BB\\_Datasheet\\_V1.pdf](http://www.evatecnet.com/sites/pdf/EVATEC_GSM1100BB_Datasheet_V1.pdf)
- [5] S. Wilbrandt, R. Leitel, D. Gäbler, O. Stenzel, N. Kaiser, "In-situ broadband monitoring and characterization of optical coatings", *Optical Interference Coatings, OSA Technical Digest Series* (2004), TuE6
- [6] W.M Duncan, S.A. Henck, J.W. Kühne, L.M. Löwenstein, S. Maung, "High-speed spectral ellipsometry for in-situ diagnostic and process control", *J.Vac.Sci. Technol. B* 12 (1994) 2779
- [7] M. Kildemo, P. Bulkin, S. Deniau, B. Drévilion, "Real time control of plasma deposited multilayers by multiwavelength ellipsometry", *Appl.Phys.Lett.* 68 (1996) 3395
- [8] C. Buzea, K. Robbie, "State of the art in thin film thickness and deposition rate monitoring sensors", *Rep.Prog.Phys.* 68 (2005) 385
- [9] S. Wilbrandt, O. Stenzel, N. Kaiser, M.K. Trubetskov, A.V. Tikhonravov, "In-situ optical characterization and reengineering of interference coatings", *Appl. Opt.* 47, (2008), C49

- [10] [http://sales.hamamatsu.com/assets/pdf/parts\\_S/s9840\\_kmpd1082e11.pdf](http://sales.hamamatsu.com/assets/pdf/parts_S/s9840_kmpd1082e11.pdf)
- [11] A.S. Kaminskii, E.L. Kosarev, E.V. Lavrov, "Using comb-like instrumental functions in high-resolution spectroscopy", *Meas.Sci.Technol.* 8 (1997), 864
- [12] A.V. Tikhonravov, M.K. Trubetskov, M.A. Kokarev, T.V. Amotchkina, A. Duparré, E. Quesnel, D. Ristau, and S. Gunster, "Effect of Systematic Errors in Spectral Photometric Data on the Accuracy of Determination of Optical Parameters of Dielectric Thin Films", *Appl. Opt.* 41, (2002), 2555
- [13] A.V. Tikhonravov, M.K. Trubetskov, T.V. Amotchkina, "Investigation of the effect of accumulation of thickness errors in optical coating production by broadband optical monitoring", *Appl. Opt.* 45 (2006), 7026
- [14] A.V. Tikhonravov, M.K. Trubetskov, "On-line characterization and reoptimization of optical coatings", *Proc. of SPIE* 5250, (2003), 406
- [15] <http://www.plasus.de/english/middle/software/specline/specline.html>